Available online at www.sciencedirect.com

ScienceDirect

Ceramics International 40 (2014) 2495–2499

CERAMICS INTERNATIONAL

www.elsevier.com/locate/ceramint

Short communication

Self-activated luminescence characteristics of double perovskite ceramic Sr_2ZrCeO_6

Cheol Woo Park[a], Hyo Jin Seo[b,*]

[a]Department of Radiological Technology, Dong-Eui Institute of Technology, Busan 614-715, Republic of Korea
[b]Department of Physics and Interdisciplinary Program of Biomedical Engineering, Pukyong National University, Busan 608-737, Republic of Korea

Received 6 June 2013; received in revised form 12 July 2013; accepted 12 July 2013
Available online 20 July 2013

Abstract

Self-activated luminescence ceramic Sr_2ZrCeO_6 were prepared via typical solid-state reaction. X-ray diffraction (XRD) and scanning electron microscope (SEM) were utilized to characterize the ceramic. The photoluminescence excitation and emission spectra, the fluorescence decay curves, X-ray-excited luminescence (XEL), Stokes shift, and CIE color coordinates were investigated. The ceramics can be efficiently excited by UV light and realize yellowish-green luminescence band peaked at 520 nm with lifetime of about 6 μs. The luminescence mechanism was discussed on the base of the luminescence properties and crystal structure. The origin of the luminescence was suggested from self-activation center of the octahedral Zr–O groups from the Zr^{4+}–O^{2-} CT transition.

Keywords: Perovskite structure; Sr_2ZrCeO_6; Charge transfer transition; Luminescence properties

1. Introduction

Compounds with perovskite ABX_3 structure are very well-known inorganic materials, which have been intensively studied in the modern solid state sciences; here A sites are larger cations, B sites are occupied by the smaller cations, and X is anion; Octahedral BX_6 groups link by the vertices and form three-dimensional frame. This forms a very large group of versatile and interesting materials, which cover conductor, semiconductor, superconductor, dielectricity (pyro-, piezo- and ferroelectric), magnetic, luminescence, photo-catalytic, energy save, etc. [1–8].

The substitution on B sites can result in double perovskite $A_2B'B''O_6$ (A being alkaline-earth, B' and B'' being two different transition metal elements). B' and B'' cations can occupy crystallographically indistinguishable sites or distinct sites depending on the charge and ionic radii. B' and B'' ions in 6-coordination are corner-shared alternately form cube-octahedral cavities, which are filled by A-site cations [9]. These materials crystallize in different type of lattices, viz., cubic, tetragonal, orthorhombic, monoclinic, etc. [10]. Double perovskites have the variety of interesting properties due to the compositional and structural diversity, which have been widely investigated for their structural, catalytic, and magnetic and microwave dielectric properties [11–13].

Perovskite-type materials have been intentionally modified by doping with rare-earth ions (RE) to enhance electrical, mechanic and magnetic properties [14–16]. RE ions doped perovskite-type materials have been widely studied in order to develop multifunctional phosphors [17], for example, perovskites of $CaTiO_3$:Pr^{3+} [18], $SrTiO_3$:Pr^{3+} [17], $BaTiO_3$:Eu^{3+} [19], and double perovskites of $Sr_2Ca(Mo,W)O_6$:Eu^{3+} [20], Sr_2CaMoO_6:Eu^{3+} [9], A_2CaWO_6 (A = Sr, Ba):Eu^{3+} [21] etc.

In this letter, of Sr_2ZrCeO_6 ceramic with double perovskite structure was prepared via typical solid-state reaction. The luminescence properties, as well as excitation and emission spectra, X-ray excited luminescence, luminescence decay etc. were reported. The luminescence mechanism was suggested on the base of the luminescence properties and crystal structure. The origin of the luminescence was suggested from self-activation center of the octahedral Zr–O groups from the Zr^{4+}–O^{2-} CT transition.

2. Experimental

Sr_2ZrCeO_6 ceramics were prepared via typical solid-state reaction method. The starting materials were stoichiometric

*Corresponding author. Tel.: +82 51 629 5568; fax: +82 51 629 5549.
E-mail address: hjseo@pknu.ac.kr (H.J. Seo).

0272-8842/$ - see front matter © 2013 Elsevier Ltd and Techna Group S.r.l. All rights reserved.
http://dx.doi.org/10.1016/j.ceramint.2013.07.061

amounts of CeO_2 (Aldrich, 99.9%), ZrO_2 (99.9%), $SrCO_3$ (Aldrich, 99.99%). The raw materials were ball-milled in alcohol for 12 h, using yttrium stabilised zirconia balls in polymeric tanks. Then the alcohol was removed by drying the milled slurry at 80 °C for 24 h in an oven. Then it was calcined in a muffle furnace at 880 °C for 4 h. The calcinated powders were dry pressed into a pellet in a steel mold. The pellets were then sintered at 1400–1450 °C for 8 h in air. For a comparison, another sample was sintered in a reducing atmosphere (CO). Both the heating rate and the cooling rate were set to 5 °C/min.

The lattice parameters and phase identification were measured by X-ray powder diffraction measurement (Philips, X'Pert-MPD System) which were collected on a Rigaku D/Max diffractometer operating at 40 kV, 30 mA with Bragg-Brentano geometry using Cu K_α radiation ($\lambda = 1.5405$ Å). The UV-excited luminescence spectra were recorded on a Perkin-Elmer LS-50B luminescence spectrometer with Monk–Gillieson type monochromators and a xenon discharge lamp used as an excitation source. The X-ray excited luminescence (XEL) spectra were measured by using an X-ray-excited spectrometer, FluorMain, where an F-30 movable X-ray tube (W anticathode target) was used as the X-ray source. Monochromators used for XEL were Monk–Gillieson type which provides the wavelength accuracy of ± 1.0 nm and the wavelength reproducibility of ± 0.5 nm. The luminescence decay curves were recorded by the 500 MHz digital storage oscilloscope (Tektronics TDS754A). The samples were excited by the forth harmonics (266 nm) of Nd-YAG pulsed laser.

3. Results

The as-prepared sample of Sr_2ZrCeO_6 ceramics at 1400 and 1450 °C were identified by powder X-ray diffraction measurements as shown in Fig. 1. The sharp peaks in each XRD pattern indicate a good crystallinity. The diffraction patterns have the same profiles with the PDF2 card number No. 54-0959 ($SrCe_{0.5}Zr_{0.5}O_3$) selected in the International Centre for Diffraction Data (ICDD) database. No impurity lines are observed, and all the reflections could be well indexed to a double perovskite single phase with space group *Pnma* (62). The lattice parameters of the samples were fitted by Jade 5.0 program as following: $a = 5.970$ Å, $b = 5.112$ Å, $c = 8.431$ Å, Volume $V = 297.586$ Å^3, formula units $Z = 4$. This is in agreement with the reported values [22].

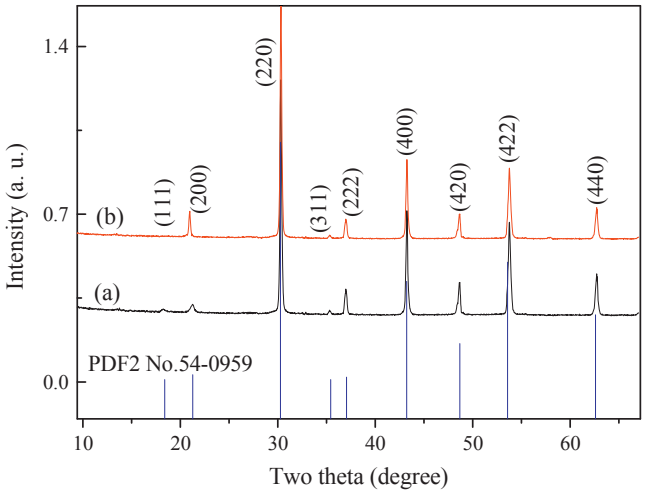

Fig. 1. The XRD patterns of Sr_2ZrCeO_6 ceramic sintered at 1400 °C (a) and 1450 °C (b) which are compared with the standard pattern card PDF2 No. 54-0959.

Fig. 2 shows the structure sketch map of the unit cell of Sr_2ZrCeO_6 crystal, which was modeled using the Diamond Crystal and Molecular Structure Visualization software on the basis of the atomic coordinate's data reported in refs [22]. Double perovskite structure Sr_2ZrCeO_6 is derived from the typical perovskite ABO_3, which is built up from ZrO_6 and CeO_6 octahedral linked together by corners, forming a three-dimensional framework as shown in Fig. 2. In the structure

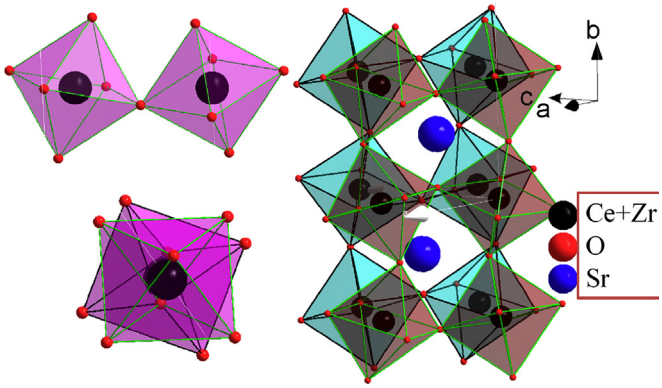

Fig. 2. The sketch map of Sr_2ZrCeO_6 crystal structure.

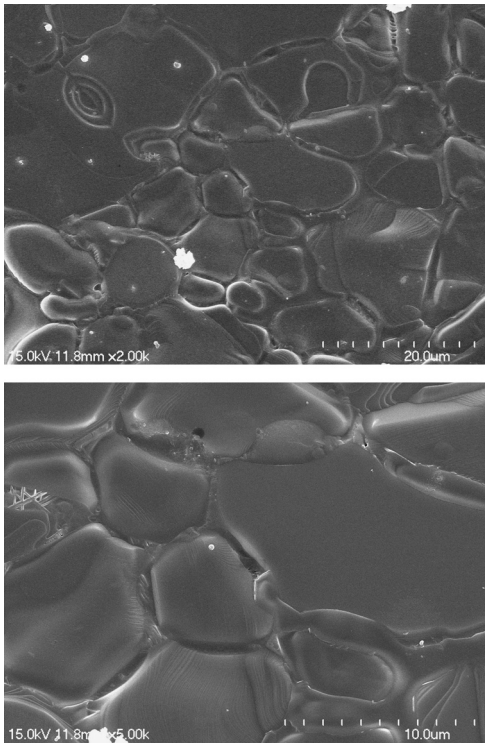

Fig. 3. The typical SEM images of Sr_2ZrCeO_6 ceramics with different amplification.

Sr^{2+} (*A*-site) ions are coordinated to 12 oxygen atoms. Octahedral site cation ordering leading to a rocksalt structure is particularly favorable when there is a large difference in oxidation state and or ionic radii of the Zr^{4+} and Ce^{4+} cations.

Fig. 3 shows the representative SEM micrograph of ceramic sample Sr_2ZrCeO_6 (1400 °C for 5 h). The ceramics show dense and well-grown grains. The ceramic particles have very fine and irregular elliptical or ball shapes with average sizes of 10 μm.

Fig. 4 presents the photoluminescence excitation (λ_{em}=520 nm) and emission (λ_{em}=315 nm) spectra of Sr_2ZrCeO_6 ceramics. The excitation spectrum by monitoring at 520 nm consists of a broad absorption band from 220 to 350 nm with a maximum at around 315 nm.

Sr_2ZrCeO_6 ceramics present green color under the excitation of UV light (250–350 nm). The emission spectrum excited by 315 nm UV light shows bright green luminescence with the maximum wavelength at 520 nm (Fig. 4). The full width at half maximum (FWHM) of the emission band is about 6100 cm^{-1}. The Stokes shift of Sr_2ZrCeO_6 luminescence can be estimated to be 12.5 × 10^3 cm^{-1}. The CIE chromaticity coordinates of luminescence in Sr_2ZrCeO_6 ceramic were calculated to be (0.311, 0.383), which are close to pure white region of the standard of National Television Standards Committee (NTSC) (x=0.33, y=0.33).

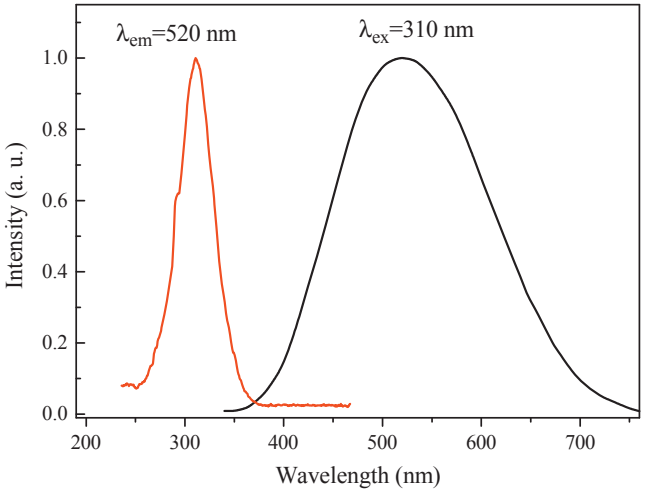

Fig. 4. The room temperature excitation (λ_{em}=520 nm) and emission (λ_{em}=315 nm) spectra of Sr_2ZrCeO_6 ceramics.

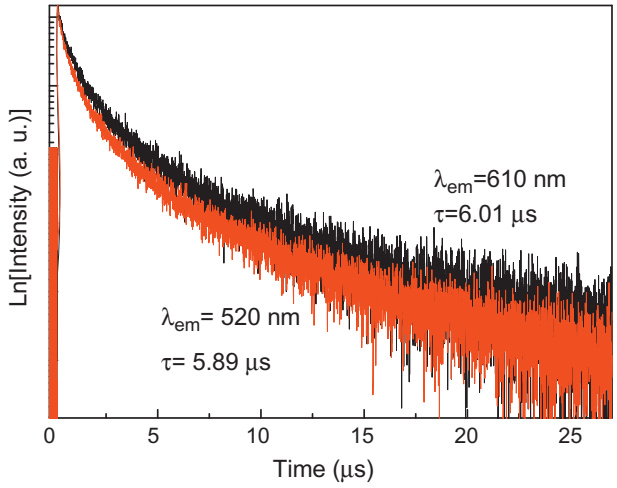

Fig. 5. The luminescence decay curves of Sr_2ZrCeO_6 ceramics by monitoring emission from 520 and 610 nm under 266 nm excitation at 300 K

The luminescence decay curves of Sr_2ZrCeO_6 ceramic under the excitation of the fourth harmonic 266 nm of a pulsed Nd: YAG laser are shown in Fig. 5; The luminescence decay curves exhibit a biexponential feature. Apparently, the two emission bands show the same luminescence decay characteristics, indicating the same dynamic emission transition from one luminescence center. The decay curves can be fitted by the equation:

$$\tau_{ave} = \frac{\int_0^\infty tI(t)dt}{\int_0^\infty I(t)dt} \quad (1)$$

where $I(t)$ is the luminescence intensity; t is the time; By fiting the curves in Eq. (1), the average decay lifetime values of 610 and 520 nm are calculated to be about 6.02 and 5.95 μs, respectively.

The luminescence of Sr_2ZrCeO_6 ceramics was also detected under excitation of X-ray; and the XEL spectrum is shown in Fig. 6. The emission shows green luminescence band centered at 525 nm with a full width at half maximum (FWHM) of 5700 cm^{-1}. Under the excitation with X-ray, the emission spectrum keeps the same profile as that under 315 nm. It is interesting that the luminescence intensities under X-ray are different from that under UV light. The sample presents very weak luminescence, which is only several percent of $Bi_4Ge_3O_{12}$ powders under the same conditions at room temperature. This indicates that the ceramics are not effective candidates as potential XEL material or scintillator.

4. Discussion

The crystal structure of double perovskite Sr_2ZrCeO_6 is derived from the typical perovskite ABO_3. $SrZrO_3$ and $SrCeO_3$

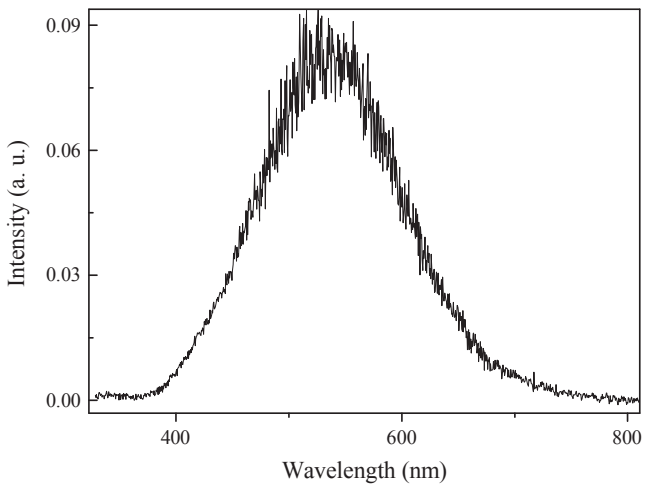

Fig. 6. The X-ray-excited luminescence spectra of Sr_2ZrCeO_6 ceramic at 300 K.

do not show any luminescence, however, efficient luminescence can be observed in Sr_2ZrCeO_6 under UV light excitation. There are several possible mechanisms for this luminescence: (1) a possible defect center; some defects such as perhaps an oxygen vacancy or a cation disorder could be formed; (2) a *d–f* transition in the excited states Ce^{3+} ions; (3) a charge transfer (CT) transition of Ce^{4+} to O^{2-}, and (4) a CT transition from Zr^{4+} to O^{2-}.

Usually, luminescence in self-activated oxides might come from the delocalization of electrons in various defect levels or energy states lying within the band gap of materials [23]. The formations of lattice defects such as oxygen-vacancies, cation vacancies etc. are possible in the solid-state reaction at high temperature. In this work, luminescence was also detected in the sample sintered in CO atmosphere; however, no difference can be found in the emission spectra from the samples sintered in air and in a reducing atmosphere (CO). This indicates that vacancy defects are not the luminescence centers responsible for the efficient luminescence.

For Ce^{3+}-based materials, a luminescence could arise from *d* to *f* transitions of Ce^{3+} ions. The *d–f* transitions in a Ce^{3+} excited state should have a lifetime of a few tenth ns. The long excited-state lifetimes (about 6.0 μs) in Fig. 5 exclude the origin of emission from *d* to *f* transitions of Ce^{3+} ions. By the way, it is necessary to get Ce^{3+} ions by sintering the raw mixtures (containing CeO_2) at high temperatures in a reducing atmosphere (N_2+H_2) or CO. In this work, the ceramics prepared by a solid-state reaction method in air are expected to be present in the form of Ce^{4+}.

In this case, is it possible that the emission in Sr_2ZrCeO_6 from a CT transition of Ce^{4+} to O^{2-}, i.e., an electron is excited from a delocalized ligand to the 4*f* shell of Ce^{4+}? It is well-known that a CT luminescence of Ce^{4+} has a very strict limitation on a crystal structure, which must be comprised of one-dimensional chains of edge-sharing CeO_6 octahedral. To date, Sr_2CeO_4 has been the only material in which the CT luminescence of Ce^{4+} is observed [24,25]. The other known Ce^{4+}-based compounds such as $SrCeO_3$ and $BaCeO_3$ each with a three-dimensional CeO_6 frame-work structure, do not have any luminescence. Sr_2ZrCeO_6 is based on an orthorhombic framework of corner-sharing ZrO_6 and CeO_6 octahedral in the structure. This implies that the luminescence in Sr_2ZrCeO_6 is very difficult from a Ce^{4+}-to-O^{2-} CT transition.

Consequentially, the excitation and fluorescence band in Sr_2ZrCeO_6 can be suggested from self-activation center of octahedral Zr–O groups by Zr^{4+}–O^{2-} CT transitions. Usually luminescence due to CT transitions from Zr^{4+} to O^{2-} in Zr^{4+} -containing compounds are located at short wavelength in UV–VUV region [26], for example, 320 nm in Sr_2ZrO_4, [27] 285 nm in $SrZrSi_2O_7$ and $BaZrSi_3O_9$ [28], 365 nm in $BaHf_{1-x}Zr_x(PO_4)_2$ [29], and 290 nm in YPO_4:Zr^{4+} [30]. However, the emission in Sr_2ZrCeO_6 (520 nm) is longer than those of the previously reported Zr^{4+}-containing compounds. Similar long wavelength emissions of Zr^{4+} are reported in β-$Zn_3(PO_4)_2$:Zr^{4+} (485 nm) [31], $Ca_3ZrSi_2O_9$ (540 nm) [26], ZrO_2 xerogel (515 nm) [32], $Ca_4ZrGe_3O_{12}$ (530 nm) [33], and $K_2YZr(PO_4)_3$ (480 nm) [34]. This difference is due to local surrounding of Zr^{4+} ions in the lattices. It has been confirmed that Zr^{4+} gives UV emission in a Zr-containing compound where the site symmetry occupied by Zr^{4+} is close to an ideal octahedron [28]. The low-energy emission (long wavelength) has been suggested to be related to the unusually disordered environments of Zr^{4+} ions in Zr-containing compounds [31].

The structure of double perovskite $A_2B'B''O_6$ is very easy to get different types of disorder in the cation or anion (or both) frameworks because of the difference between $B'O_6$ and $B''O_6$ octahedral. For a perovskite the tolerance factor, τ, gives a measure of the fit of the larger *A*-site cation to the cubic framework of corner connected octahedral. When τ falls below unity, the octahedral tilting distortions are expected [35].

Fig. 2 is the schematic picture of double perovskite Sr_2ZrCeO_6. Zr^{4+} (r=0.72 nm CN=6) and Ce^{4+} (r=1.01 nm CN=6) ions on *B*-sites have obvious octahedral tilting because of the difference between their ionic radius, i.e., one rotates clockwise, and another rotates counterclockwise. It could be suggested that the disorder of Zr^{4+} sites in Sr_2ZrCeO_6 lattices could bring unusual luminescence, i.e., long wavelength emission. Similar situation can be found in the other transition-metal oxides. For example, blue and green emission bands in niobates are due to two different niobate centers, *viz*, a regular and a defect niobate center [36]. Usually the efficient blue emission originates from the regular niobate center and the weaker green emission from the defect niobate center [37].

5. Conclusions

Sr_2ZrCeO_6 ceramics were prepared via typical solid-state reaction, which can crystallize in fine grains with average sizes of 10 μm. The luminescence properties and luminescence mechanism were suggested. The ceramics can be excited by UV light (220 to 350 nm) and X-ray irradiations. The emission of Sr_2ZrCeO_6 ceramics shows bright green luminescence with the maximum wavelength at 520 nm and CIE color coordinates of x=0.311, y=0.383. The Stokes shift was estimated to be 12.5×10^3 cm^{-1}. The sample presents one luminescence center with average decay time value of about 6.0 μs. The luminescence of double perovskite Sr_2ZrCeO_6 is unusual, i.e., it is at longer wavelength than those of the previously reported Zr^{4+}-containing compounds. The unusual self-activated luminescence in Sr_2ZrCeO_6 might be related to the disturbed environment of Zr^{4+} ions in the lattice. To elucidate the detailed luminescence mechanism of perovskite Sr_2ZrCeO_6, investigations will be conducted in the future.

Acknowledgment

This research was supported by Basic Science Research Program through the National Research Foundation of Korea (NRF) funded by the Ministry of Science, ICT & Future Planning (NRF-2013-R1A1A2009154).

References

[1] Y.M. Huang, L.J. Liu, D.P. Shi, S.S. Wu, S.Y. Zheng, L. Fang, C.Z. Hu, B. Elouadi, Giant dielectric permittivity and non-linear electrical behavior in $CaCu_3Ti_4O_{12}$ varistors from the molten-salt synthesized powder, Ceramics International 39 (2013) 6063–6068.

[2] S. Thakur, O.P. Pandey, K. Singh, Structural and dielectric properties of $Bi_{1-x}Sr_xMnO_3$ ($0.40 \le x \le 0.55$), Ceramics International 39 (2013) 6165–6174.

[3] X. Xue, G.Q. Tan, H.J. Ren, A. Xia, Structural, electric and multiferroic properties of Sm-doped $BiFeO_3$ thin films prepared by the sol–gel process, Ceramics International 39 (2013) 6223–6228.

[4] D.Y. Lu, L. Zhang, X.Y. Sun, Defect chemistry of a high-k 'Y_5V' $(Ba_{0.95}Eu_{0.05})TiO_3$ ceramic, Ceramics International 39 (2013) 6369–6377.

[5] S. Chauhan, M. Arora, P.C. Sati, S. Chhoker, S.C. Katyal, M. Kumar, Structural, vibrational, optical, magnetic and dielectric properties of $Bi_{1-x}Ba_xFeO_3$ nanoparticles, Ceramics International 39 (2013) 6399–6405.

[6] D.K. Lim, B. Singh, J. Kang, J. Kim, S.J. Song, Study of electrochemical hydrogen charge/discharge properties of $FePO_4$ for application as negative electrodes in hydrogen batteries, Ceramics International 39 (2013) 6559–6568.

[7] T. Chen, H.L. Wang, T. Zhang, G.C. Wang, J.F. Zhou, J.W. Zhang, Y. H. Liu, Piezoelectric behavior of $(1-x)K_{0.50}Na_{0.50}NbO_{3-x}Ba_{0.80}Ca_{0.20}ZrO_3$ lead-free ceramics, Ceramics International 39 (2013) 6619–6622.

[8] T. Wei, Q.J. Zhou, C.Z. Zhao, Y.B. Lin, Y.L. Zou, Y. Li, L.S. Zhang, Strong green light emission in Ho doped $Bi_4Ti_3O_{12}$ ferroelectric ceramics, Ceramics International 39 (2013) 7211–7215.

[9] V. Sivakumar, U.V. Varadaraju, A promising orange–red phosphor under near UV excitation, Electrochemical and Solid-State Letters 9 (2006) H35–H38.

[10] P.W. Barnes, M.W. Lufaso, P.M. Woodward, Structure determination of $A_2M^{3+}TaO_6$ and $A_2M^{3+}NbO_6$ ordered perovskites: octahedral tilting and pseudosymmetry, Acta Crystallographica Section B: Structural Science 62 (2006) 384–396.

[11] A. Dias, M. Lage, L.A. Khalam, M.T. Sebastian, R.L. Moreira, Vibrational spectroscopy of Ca_2LnTaO_6 (Ln = lanthanides, Y, and In) and Ca_2InNbO_6 double perovskites, Chemistry of Materials 23 (2011) 14–20.

[12] L.A. Khalam, M.T. Sebastian, Effect of cation substitution and non-stoichiometry on the microwave dielectric properties of $Sr(B'_{0.5}Ta_{0.5})O_3$ [B′ = lanthanides] perovskites, Journal of the American Ceramic Society 89 (2006) 3689–3695.

[13] B. Manouna, S. Benmokhtarb, L. Biha, M. Azroura, A. Ezzahic, A. Iderc, M. Azdouza, H. Annerstend, P. Lazor, Synthesis, structure, and high temperature Mössbauer and Raman spectroscopy studies of $Ba_{1.6}Sr_{1.4}Fe_2WO_9$ double perovskite, Journal of Alloys and Compounds 509 (2011) 66–71.

[14] S.B. Reddy, K.P. Rao, M.S.R. Rao, Influence of *A*-site Gd doping on the microstructure and dielectric properties of $Ba(Zr_{0.1}Ti_{0.9})O_3$ ceramics, Journal of Alloys and Compounds 509 (2011) 1266–1270.

[15] X. Cheng, Y. Li, F. Kong, L. Li, Q. Sun, F. Wang, Red, green, blue and bright white upconversion luminescence of $CaTiO_3:Er^{3+}/Tm^{3+}/Yb^{3+}$ nanocrystals, Journal of Alloys and Compounds 541 (2012) 505–509.

[16] S.K. Jo, J.S. Park, Y.H. Han, Effects of multi-doping of rare-earth oxides on the microstructure and dielectric properties of $BaTiO_3$, Journal of Alloys and Compounds 501 (2010) 259–264.

[17] H. Yamamoto, S. Okamoto, H. Kobayashi, Luminescence of rare-earth ions in perovskite-type oxides: from basic research to applications, Journal of Luminescence 100 (2002) 325–332.

[18] A. Vecht, D.W. Smith, S.S. Chadha, C.S. Gibbons, J. Koh, D. Morton, New electron excited light-emitting materials, Journal of Vacuum Science and Technology B 12 (1994) 781–784.

[19] S. Fuentes, N. Barraza, E. Veloso, R. Villarroel, J. Llanos, Effects of Eu substitution on luminescent and magnetic properties of $BaTiO_3$ nanomaterials, Journal of Alloys and Compounds 569 (2013) 52–57.

[20] S. Ye, C.H. Wang, X.P. Jing, Photoluminescence and raman spectra of double-perovskite $Sr_2Ca(Mo/W)O_6$ with *A*- and *B*-site substitutions of Eu^{3+}, Journal of the Electrochemical Society 155 (2008) J148–J151.

[21] V. Sivakumar, U.V. Varadaraju, Synthesis, phase transition and photoluminescence studies on Eu^{3+}-substituted double perovskites—a novel orange–red phosphor for solid-state lighting, Journal of Solid State Chemistry 181 (2008) 3344.

[22] A.E. Solovieva, A.M. Gavrish, E.I. Zoz, X-ray investigation of the solid solutions in the system $SrCeO_3$–$SrZrO_3$, Inorganic Materials 10 (1974) 402–404.

[23] M. Bharathy, V.A. Rassolov, H.C. zur Loye, Crystal growth of Sr_3NaNbO_6 and Sr_3NaTaO_6: new photoluminescent oxides, Chemistry of Materials 20 (2008) 2268–2273.

[24] E. Danielson, M Devenney, D.M. Giaquinta, J.H. Golden, R.C. Haushalter, E.W. McFarland, D.M. Poojary, C.M. Reaves, W.H. Weiberg, X.D. Wu, A rare-earth phosphor containing one-dimensional chains identified through combinatorial methods, Science 279 (1998) 837–839.

[25] L. Li, S.H. Zhou, S.Y. Zhang, Investigation on charge transfer bands of Ce^{4+} in Sr_2CeO_4-blue phosphor, Chemical Physics Letters 453 (2008) 283–289.

[26] G. Blasse, G. Bernardi, D.J.W. IJdo, J.R. Plaisier, Yellow zirconate luminescence in $Ca_3ZrSi_2O_9$, Journal of Alloys and Compounds 217 (1995) 29–30.

[27] L. Zhang, G.Y. Hong, X.L. Sun, The luminescence of the phosphor Sr_2ZrO_4 with one-dimensional chains structure, Chinese Chemical Letters 10 (1999) 799–802.

[28] G. Blasse, W.J. Schipper, M.E. Huntelaar, D.J.W. Ijdo, Luminescence of $SrZrSi_2O_7$, Journal of Physics and Chemistry of Solids 54 (1993) 1001–1003.

[29] C.R. Miao, C.C. Torardi, A new high-efficiency UV-Emitting X-ray phosphor, $BaHf_{1-x}Zr_x(PO_4)_2$, Journal of Solid State Chemistry 155 (2000) 229–232.

[30] M. Kaneyoshi, E. Nakazawa, Luminescence of YPO_4:Zr and YPO_4:Zr, Mn under vacuum ultraviolet excitation, Journal of the Electrochemical Society 152 (2005) H80–H83.

[31] J. Wang, S. Wang, Q. Su, Luminescence and defect properties of novel bluish-green phosphor β-$Zn_3(PO_4)_2:Zr^{4+}$, Journal of Rare Earth 22 (2004) 83–86.

[32] M. Pan, J.R. Liu, P. Yang, M.K. Lu, D. Xu, D.R. Yuan, D.R. Chen, Strong luminescence of pure and yttrium doped zirconia xerogels, Journal of Materials Science Letters 20 (2001) 1565–1567.

[33] G. Blasse, J.D. Blank, D.J.W. Ijdo, The luminescence of the garnet $Ca_4ZrGe_3O_{12}$, Materials Research Bulletin 30 (1995) 845–850.

[34] L. Shi, H.J. Seo, Tunable white-light emission in single-phased $K_2Y_{1-x}Eu_xZr(PO_4)_3$ phosphor, Optics Express 19 (2011) 7147–7152.

[35] S.G. Martin, G. King, E.U. Garrote, G. Nenert, P.M. Woodward, Spontaneous superlattice formation in the doubly ordered perovskite $KLaMnWO_6$, Chemistry of Materials 23 (2011) 163–170.

[36] A.J.H. Macke, Luminescence in the system $Mg_4Ta_{2-x}Nb_xO_9$, Journal of Solid State Chemistry 19 (1976) 221–226.

[37] M. Wiegel, M. Hamoumi, G. Blasse, Luminescence and nonlinear-optical properties of perovskite-like niobates and titanates, Materials Chemistry and Physics 36 (1994) 289–293.